ACS NANO

www.acsnano.org

LETTER TO THE EDITOR

Reply to Comment on Conopeptide-Functionalized Nanoparticles Selectively Antagonize Extrasynaptic *N*-Methyl-D-aspartate Receptors and Protect Hippocampal Neurons from Excitotoxicity *In Vitro*

Pierluigi Valente,[‡] Darya Kiryushko,[‡] Silvio Sacchetti, Pedro Machado, Claire M. Cobley, Vincenzo Mangini, Alexandra E. Porter, Joachim P. Spatz, Roland A. Fleck, Fabio Benfenati, and Roberto Fiammengo*

Cite This: *ACS Nano* 2021, 15, 15409–15417

Read Online

ACCESS | Metrics & More | Article Recommendations

We recently described conopeptide-functionalized gold nanoparticles (AuNPs) that can be used to selectively antagonize extrasynaptic *N*-methyl-D-aspartate receptors (NMDARs), resulting in neuroprotection against excitotoxicity *in vitro*.[1] In that paper, we acknowledged that the Molokanova group was the first to provide evidence that AuNPs functionalized with NMDAR antagonists (memantine) could be used to antagonize extrasynaptic NMDARs.[2] To achieve their excellent results, they exploited AuNPs coated with thiol-terminated poly(ethylene glycol) on top of which the NMDA receptor antagonist memantine was bound through a covalent bond. We are slightly dismayed that our article has originated the concerns expressed in Molokanova's comment, as our system is based on similar materials. Actually, at the time their manuscript appeared, we were already working on the system[3,4] recently published in *ACS Nano*,[1] although with different collaborators. Note also that we had made the idea available to the scientific community before Dr. Molokanova submitted her patent application (2013-11-05, priority to US201361962335P) and long before they submitted their *Nano Letter* article (received 2016-05-16). In fact, in the outlook of the *ACS Nano* article published in 2010 it is written: "*Conjugation of peptide-based NMDA receptor antagonists to AuNPs could be used to spatially restrict NMDA-receptor blockade to specific cellular locations and may be suitable to specifically block extrasynaptic NMDA receptors that promote cell death pathways and neurodegeneration*".[3] Moreover in a *Nature Reviews Neuroscience* article published by my former collaborator Hilmar Bading in August 2013, it is also written: "*Selective blockade of e-NMDARs may also be possible by attaching an NMDAR blocker to a nanoparticle. If the size of the nanoparticle exceeds that of the synaptic cleft, the blocker can only target e-NMDARs while sparing synaptically localized NMDARs*".[5] Our preliminary observations were in agreement with the data reported by Molokanova *et al.*[2] and were later confirmed and expanded as shown in our *ACS Nano* article.[1] The substantial agreement between these two studies is a reassuring scientific aspect, as it proves the validity of the approach, that is, PEGylated AuNPs carrying NMDAR antagonists, with an overall dimension large enough to prevent their diffusion into the synapse, exclusively antagonize extrasynaptic NMDAR-mediated currents and are thereby neuroprotective.

STABILITY OF CONOPEPTIDE-FUNCTIONALIZED AUNPS

A major issue raised by Molokanova's comment is the "structural stability" of our nanoparticles. In particular, the authors express concerns about the release in solution of the NMDAR antagonists conantokin-G (Con-G′*) or conantokin-R (Con-R′*), which are covalently bound to the PEG-based AuNP coating.[1] This aspect is indeed crucial and was specifically addressed through careful material and experimental design as well as by implementing several levels of control, which are detailed in the following paragraphs.

Stability of the Passivation Layer. The antagonists Con-G′* and Con-R′* are covalently bound through a heterobifunctional linker to the AuNP passivation layer made of a

Received: July 1, 2021
Published: October 26, 2021

self-assembled monolayer (SAM) of alkyl-PEG600 thiols.[3] In contrast to more commonly employed thiolated PEGs, the presence of a long alkyl chain of 11 carbon atoms between the thiol group and the PEG segment completely suppresses thiol displacement reactions and effectively shields the Au surface.[3,6−8] This property is fundamental in the design of our AuNP-based NMDAR antagonist to ensure structural stability of the conjugates, because thiol displacement would result in antagonist release in solution.

Use of Fluorescently Labeled Antagonists (with No Loss of Activity). We purposely chose to coat our AuNPs with SAMs characterized by proven superior stability toward thiol displacement. However, we built in the system the possibility to monitor antagonist release by using fluorescently labeled derivatives Con-G* and Con-R′*. The fluorophore carboxytetramethylrhodamine (TAMRA) was linked to the $N(\varepsilon)$ of the single Lys residue close to the C-terminus of both peptides. It is well-known that, to maintain the biological activity of conantokins, it is important to leave their N-terminus unmodified.[9] Indeed, we directly compared the activity of labeled *vs* unlabeled peptides under our experimental conditions and found no significant difference in their neuroprotective activity (see Figure S3 in ref 1).

Control of the Purification Procedure for the Antagonist-AuNP Conjugates. The fluorescent label allowed us to assess the efficacy of the cleaning procedure after conjugation. The excess of unconjugated peptides in solution was removed down to ≤2 ± 2 free peptides/AuNP. The purification procedure detailed in the Supporting Information of the manuscript consisted of several ultrafiltration steps followed by a final gel filtration step. The eluted AuNP solutions were centrifuged, and the supernatants used to measure the residual amount of fluorescence in solution. At the end of the preparation, a 50 μL aliquot of the AuNP solution was centrifuged to pellet the nanoparticles, and the fluorescence of the supernatant was measured after 200-fold dilution. This approach makes it feasible to measure very small amounts of peptides free in solution. Direct quantification of the average number of peptides/AuNP was carried out using the procedure described in the manuscript and reported previously.[10] This procedure requires a nanoparticle sample dilution in the range of 500−1000 times.

Control of the Release of Peptides upon Prolonged Storage. The approach described in the previous paragraph was used to quantify peptide release upon storage, which resulted in <10% after 28 days as clearly stated in manuscript, when the AuNP samples were aliquoted and stored in the dark at 4 °C until use. To support our statement, we show here the release of fluorescence in solution over time for two nanoparticle batches as a measure of peptide release from the conjugates (Figure 1).

These data do not contradict our previous data[10] reporting a loss of approximately 25% of the peptides after 14 days, which further increased to 35% after 42 days, because those samples were stored at *room temperature* and were *not aliquoted*, which is important to minimize oxygenation of the AuNP solutions. In fact, several authors have demonstrated that SAMs of (PEG)thiols on Au deteriorate over time due to oxidation of the thiol group, resulting in adsorbate desorption.[11−13] Accordingly, no matter how the antagonist is bound to the PEG-termini, such occurrence would result in antagonist release in solution allowing its free diffusion. Thus, to ensure structural stability of the conopeptide-functionalized gold

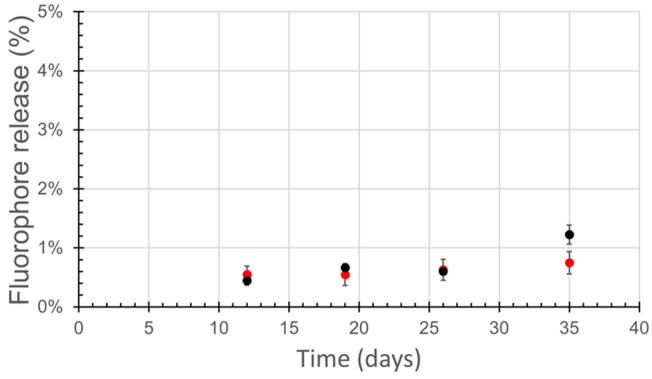

Figure 1. Release of fluorescently labeled peptides in solution over time from Con-G′*-AuNPs 1 or Ctrl AuNPs 2. Only a very small percentage of fluorophore is release in solution over time for Con-G′*-AuNPs 1 (red circles) or Ctrl AuNPs 2 (black circles). The amount of fluorophore is indicative of the antagonistic peptides released in solution, as we used fluorescently labeled peptides to functionalize the AuNPs.[1] AuNP samples were aliquoted and stored in the dark at 4 °C directly after preparation and until use. 50 μL aliquots of AuNP solution were centrifuged 40 min at 14000×*g* and 4 °C to pellet the nanoparticles. The fluorescence of the supernatant was then measured after 200-fold dilution, and the fluorophore was quantified by comparison with a calibration line. The total amount of fluorophore on the nanoparticles was measured after stripping off the passivation layer and the peptides from the AuNP surface with DTT-PB buffer (1 M 1,4-dithiothreitol in 0.18 M sodium phosphate buffer pH 8.0) as previously reported.[10] Error bars are standard deviations of triplicate measurements on one AuNP batch.

nanoparticles (AuNPs **1**−**3**), the time frame of the *in vitro* experiments took place between 1 and 4 weeks after their preparation. The nanoparticles needed for multiple experiments were aliquoted upon arrival to minimize unnecessary manipulations and stored in the dark at 4 °C. It is important to note that these precautions are not specific to our AuNP system but deemed necessary for any type of AuNP passivated with SAMs of (PEG)thiols to be used for biological applications, including those developed by the Molokanova group.

Choice of the Most Suitable AuNP Concentration for *In Vitro* Experiments. Activity experiments with Con-G*-AuNPs **1** were run at a concentration of 0.25 nM to maximize the chances of obtaining clear, robust results. As reported in the manuscript, "*... in the unlikely event that all peptides become detached from the AuNPs during the experiment ...*", and in the absence of peptide degradation in the biological media "*... the maximum reachable free peptide concentration starting from 0.25 nM AuNPs**1** would be below ∼60 nM, which is too small to antagonize NMDAR activity (49)*". This is exactly the opposite of Dr. Molokanova's claim: "*Thus, the effects in biological (including, neuroprotective) studies could be, at least partly, due to detached "free" conopeptides rather than from intact nanoconjugates ...*" Yet, the results in Figure S3 show that neuroprotection can be observed only with Con-G (peptide free in solution) concentrations ≥100 nM, but not at 10 nM, demonstrating that the effect observed in our experiments cannot be ascribed to detached "free" conopeptides. Considering the electrophysiology recordings, our results provide direct evidence that antagonist activity is not due to free peptides. NMDAR-mediated evoked excitatory postsynaptic currents (eEPSCs, purely synaptic events) measured in

https://doi.org/10.1021/acsnano.1c05607
ACS Nano 2021, 15, 15409−15417

the same cell before (I1) and during (I2) treatment with AuNPs are not significantly different (Figure 4e,f). This means that no synaptic-NMDAR antagonist activity is measured following particle application, ruling out the possibility that the observed outcomes are due to free antagonist. Thus, the significant antagonistic activity of Con-G′*-AuNPs **1** (or Con-R′*-AuNPs **3**, but not of Ctrl AuNPs **2**), observed on total NMDA-gated current from the same neuron just a few minutes later, is due to extrasynaptic NMDAR inhibition. As an additional control, we preincubated neurons for 1 h with Con-G′*-AuNPs **1** and ran the same electrophysiology recordings shown in Figure 4e. The results show that the observed NMDA-gated current is not significantly different from the one obtained after only 1 min incubation, suggesting that extrasynaptic NMDARs were quickly antagonized and that the antagonist activity of our conjugates was retained for up to 1 h. Finally, 0.25 nM of conopeptide-functionalized AuNPs cannot be claimed a "low" antagonist concentration. For all AuNP batches used in our study, peptide loading was higher than 100 peptides/AuNP. This degree of functionalization ensured a high local concentration of antagonist of approximately 1.5 mM (calculated for 120 peptides attached to nanoparticles with a hydrodynamic diameter of 60 nm) irrespective of the applied nanoparticle concentration. The possibility of achieving high local concentration of a ligand, or forced proximity, governs the interaction between multivalent scaffolds and their target, resulting in increased affinity.[14−17] Since the reported affinities for free Con-G and Con-R are in the low micromolar range,[18] experiments run at 0.25 nM AuNPs are likely to be at a saturating antagonist concentration for all NMDARs *that are reached physically* by these nanoparticles.

In summary, the biological activity experiments were designed in such a way that any structural instability of the conjugates would result in no observable or minimal antagonism. Importantly, the same goal cannot be reached performing the experiments at higher AuNP concentrations, because the observed effects may indeed be partially due to released antagonists, which would be at a sufficiently high concentration, as suggested by Molokanova and co-worker in their comment.

To avoid misunderstandings, we would like to clarify how AuNP concentration was determined. According to transmission electron microscopy (TEM), the AuNPs prepared for this study can be approximated to spheres whose diameter can be obtained from the TEM images. In detail, our AuNPs have narrow, Gaussian-shaped size distributions as shown in Figure S1b,c,[1] with small standard deviation (<10%), which justifies considering them as monodisperse. The average ellipticity of these nanoparticles, defined as the ratio between major and minor axes, was ≤1.11, supporting the assumption of spherical shape. This is a proven, common assumption in the field of AuNPs.[19,20] The concentration of gold in solution (after AuNPs have been dissolved with aqua regia) can be measured *via* ICP-OES or another suitable quantitative elemental analysis technique. Thus, nanoparticle concentration can be calculated from the concentration of gold, considering the nanoparticles as spheres whose diameter equals the average value from the size distribution determined *via* TEM. This procedure is a standard practice in AuNP research but can be used for other materials as well.

FUNCTIONAL ASPECTS

Both our study and the Molokanova's study originate from the need of new approaches for the selective inhibition of extrasynaptic NMDARs, because this result cannot be achieved with more traditional, small molecule antagonists, given the substantially similar pharmacological profiles of synaptic and extrasynaptic NMDARs.[21]

Conopeptide-Functionalized AuNPs and Synaptic NMDARs. The authors of the comment express concerns about the activity of our conopeptide-functionalized AuNPs on synaptic NMDARs. We underline the paramount importance of performing experiments at "low" AuNP concentration to ensure that the observed antagonist activity can be only due to the conjugates and not to the exceedingly low concentrations of free antagonists, should they be present. On the contrary, working at high AuNP concentration carries the risk that the observed activity may be spurious and partially contributed by released antagonist peptides. Under the reported experimental conditions, Con-G′*-AuNPs **1** and Con-R′*-AuNPs **3** did not antagonize synaptic NMDARs (Figures 3 and 4f[1]). As a central point of this study, the lack of antagonism on synaptic NMDARs was demonstrated with two, independent, electrophysiological protocols, namely: (1) recording miniature excitatory postsynaptic currents (mEPSCs) in low-density hippocampal neuron cultures, and (2) recording evoked excitatory postsynaptic currents (eEPSCs) in autaptic hippocampal neurons. At the same concentration, our AuNPs inhibited 20−30% of the total NMDAR-dependent current in autaptic hippocampal neuron cultures, corresponding to approximately 2/3 of the calculated extrasynaptic current (from Figure 4g[1]). The lack of antagonism on synaptic NMDARs can only be explained by the inability of the conjugates to reach this receptor population, because of their size, as confirmed by TEM analysis. The inhibitory effect on the extrasynaptic NMDAR population also demonstrates that antagonist peptides retained activity when bound to the nanoparticles. Altogether, our results show that, under the reported experimental conditions, conopeptide-functionalized AuNPs can antagonize specifically and exclusively (a fraction of) extrasynaptically located NMDARs because their large size prevents them from reaching synaptically located receptors.

The results of our TEM study supported this hypothesis. As reported in the manuscript, large data sets were generated by sectioning the samples at random positions in the coverslip and then imaging 450 fields of view. For each image displaying both AuNPs and synapses, we computed the distance of each AuNP from the synapse center, which resulted in 211 AuNP-synapse distances for AuNPs **1** and 366 distances for AuNPs **3**. The shortest AuNP-synapse distances ranged between 217 and 300 nm, demonstrating that AuNPs and synapses are not colocalized (Figure 2[1]). Scale bars shown on each image are 200 nm, although we apologize to the readers for missing reference to it in the caption. The images show, in some cases, clusters of few AuNPs (3−8), as noted in Molokanova's comment, which are possibly indicative of targeting of NMDARs that are spatially close. This explanation agrees well with older studies showing that NMDARs at extrasynaptic locations are clustered.[22] However, these images cannot be used to infer tendency toward nanoparticle aggregation because of poor colloidal stability. We have previously shown that AuNPs passivated with alkyl-PEG600 thiols do not aggregate in DMEM cell culture medium for more than 24 h,

https://doi.org/10.1021/acsnano.1c05607
ACS Nano 2021, 15, 15409−15417

based on UV−vis measurements.[3] To dismiss all doubts in this respect, we show here the dynamic light scattering (DLS) measurements of Con-G′*-AuNPs **1** in the cell culture medium used for the hippocampal neurons, and for their treatment with nanoparticles, which demonstrate that aggregation does not occur (see Figure 2), contrary to the claim by Molokanova *et al.*

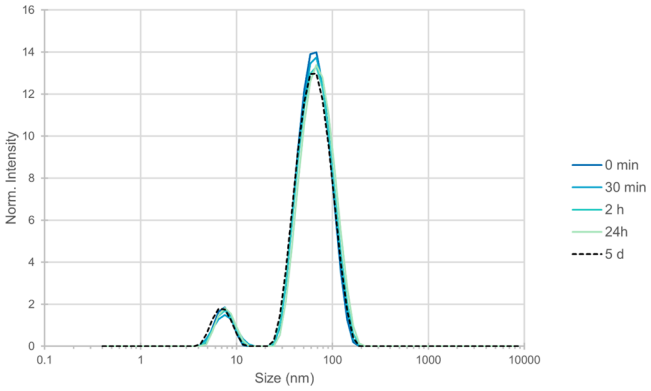

Figure 2. Evolution of DLS size distribution over time for Con-G′*-AuNPs 1 dispersed in neurobasal medium +10% B27 supplement. Con-G′*-AuNPs 1 do dot aggregate when suspended in neurobasal medium supplemented to reach a final concentration of 5% glutamax, 5% penicillin/streptomycin, and 10% B-27 supplement, the cell culture medium used for hippocampal neuron culture in our manuscript.[1] This medium contains proteins (in the B-27 supplement), the most abundant of which is bovine serum albumin (BSA, the peak at ∼8 nm).[23] The hydrodynamic diameter of Con-G′*-AuNPs 1 in this medium is ∼69 nm (60 ± 3 in 10−50 mM $NaHCO_3$, pH 8.4, Table 1[1]).

The comment also suggests testing antagonist-functionalized nanoparticles that can freely diffuse into the synaptic cleft. However, it is important to note that even particles with cores below 10 nm diameter will probably be too large to reliably enter the synapse due to the alkyl-PEG600 chains, which always add 6−8 nm to the AuNP hydrodynamic diameter, making the results of such experiments difficult to interpret. It is also unclear what kind of additional information such nanoparticles would add to the overall picture since our experiments already demonstrate that the peptides retain their antagonist activity when bound to the nanoparticles, as discussed above. Both nanoparticle size and synaptic cleft width are distributed around the average values indicated in the manuscript. We show that in our nanoparticle-based NMDAR-antagonist formulations, practically all nanoparticles are larger than 20 nm, as evident from their TEM and DLS size distribution (Figure S1[1]). We deliberately used such "large" nanoparticles as a precautionary measure to lower the probability of diffusion into the synaptic cleft, whose width distribution is centered on 25 nm.[24,25] While we do not have indications about the diffusion properties of our nanoparticles within brain tissue *in vitro* or *in vivo* (because all our experiments were conducted on cultured cells), it seems reasonable to assume no major obstacles based on the data reported by other groups.[26] However, this point definitely deserves further attention if aiming at a therapeutic clinical application.

Finally, the suggestion that lack of antagonist activity on synaptic NMDARs observed from electrophysiology recordings at 0.25 nM AuNP concentration may not be indicative of the actual situation during neuroprotection experiments is unwarranted. Likewise, it is not factual to imply that the observed neuroprotection may be due to antagonist released in solution. The neuroprotective effect of Con-G′*-AuNPs **1** was statistically significant at nanoparticle concentrations ≥0.5 nM (Figure 5a[1]), while for Con-R′*-AuNPs **3** concentrations as low as ≥0.1 nM already produced a statistically significant effect (Figure 5c[1]). Thus, only for Con-G′*-AuNPs **1**, the concentration at which significant neuroprotection is observed is just 2-fold higher than the concentration used in electrophysiology, while for Con-R′*-AuNPs **3**, it is lower. As already discussed above, we have shown in a control experiment that the inhibited NMDA-gated currents were not significantly different whether neurons were preincubated with Con-G′*-AuNPs **1** for 1 min or for 1 h (Figure 4g,h[1]). This result is not in agreement with an extensive release of active (undegraded) peptides in solution. Even at the highest concentration tested in the neuroprotection experiments (1 nM), one would need the release of roughly half of the conjugated Con-G to observe some biological activity.

In the manuscript, we pointed out that we observed a statistically significant reduction in mEPSCs frequency in the presence of AuNPs **1** (Figure 3c[1]) compared to the untreated sample, likely attributable to decreased resting intracellular calcium ($[Ca^{2+}]_i$). While we still do not know the origin of this effect, it is not compatible with partial inhibition of synaptic NMDARs because mEPSCs amplitude and resting potential were unaffected. Unfortunately, an analogous comparison is missing in Molokanova's paper,[2] but a look at the electrophysiology recording shown in their Figure 3b[2] hints at a reduction in mEPSCs frequency upon treatment with both memantine-functionalized AuNPs (AuM) and memantine alone (Figure 3c[2]).

Conopeptide-Functionalized AuNPs and Extrasynaptic NMDARs. We have extensively discussed and motivated the choice of low AuNP concentration (0.25 nM) for our electrophysiology recordings. The lack of inhibition of synaptic activity is demonstrated with two, completely independent, recording protocols. In case of eEPSCs—pure synaptic events—the protocol shown in Figure 4e[1] allows *direct* evidence, cell by cell, that our AuNPs do not inhibit synaptic currents, while they cause a statistically significant inhibition of total (synaptic + extrasynaptic) NMDA-gated currents. This reliable experimental paradigm allows to study the effects of extrasynaptic NMDARs activity modulation and at the same time monitors synaptic NMDAR activity. The alternative pharmacological isolation protocol relies on the irreversible blockade of synaptic NMDARs with MK801 during hyperactivity (even if some objections to this view have appeared)[27] to be able to address specifically extrasynaptic receptors. The two protocols follow distinct strategies, with pros and cons, but both can be considered reliable. Moreover, our protocol includes all the appropriate and necessary controls. For each neuron, we first measured the eEPSC upon brief depolarization of the cell body to +40 mV for 0.5 ms applied at 0.1 Hz for about 120 s to stabilize the eEPSC amplitude. We then repeated the same measure after perfusion of the cell under study with the AuNPs, confirming the absence of antagonistic activity on the synaptic currents (*i.e.*, I2 = I1 Figure 4e-f,[1] the numbers of cells are those reported in panel 4g). Finally, still in the presence of AuNPs, we applied NMDA to open the NMDAR channels not blocked by the nanoparticles, that is, synaptic NMDARs + a fraction of the extrasynaptic ones,

https://doi.org/10.1021/acsnano.1c05607
ACS Nano 2021, 15, 15409−15417

affording current I3. For a given neuron the difference I3−I2 corresponds to the current flowing through the fraction of extrasynaptic NMDARs that are not blocked by AuNPs. This contribution is normalized by I3 to allow the comparison between groups of treated neurons (Figure 4g[1]). In case of vehicle-treated neurons, I3 is the total NMDAR-mediated current (synaptic + extrasynaptic) and (I3 − I2)/I3 is the normalized extrasynaptic current component. In case of complete extrasynaptic inhibition, I3 = I2, and therefore the normalized extrasynaptic current is null. In all other cases, (I3 − I2)/I3 is larger than the actual extrasynaptic current because I3 < $I3_{veh}$. In other words, (I3 − I2)/I3 is an overestimation of the normalized extrasynaptic current. Thus, while a reduction of (I3 − I2)/I3 for AuNP-treated compared to vehicle-treated cells indicates extrasynaptic current inhibition (Figure 4g[1]), this approach underestimates the actual degree of inhibition. Yet, it has two main advantages: (1) it allows direct measure of the synaptic component during AuNP treatment within the very same recording, and (2) it underestimates the degree of inhibition of the extrasynaptic component, thereby reducing the possibility of false positives. Finally, the results obtained for each group of differently treated cells are compared and statistically analyzed.

To summarize, we have developed an alternative testing protocol applicable to antagonists whose free diffusion in the synapse is hindered, as is the case of our AuNPs or the one developed by the Molokanova's group. This protocol can show the absence of synaptic NMDAR inhibition but does not allow direct quantification of extrasynaptic NMDARs inhibition alone. Yet, its validity is supported by the results obtained with the electrophysiology recordings shown in Figure 4a.[1] Overall, these experiments indicate that treatment with conopeptide-functionalized AuNPs antagonize (at least partially) extrasynaptic NMDARs while allowing synaptic NMDARs activity, a situation considered necessary for any possible future pharmaceutical development in this field.

As noted above, the synaptic currents measured before (I1) and after (I2) AuNP application are not significantly different, that is, their ratio is around 1. However, we have reported their absolute values (and not their ratio) in Figure 4f[1] as additional information to appreciate that all patch-clamped cells we tested were showing initial comparable currents. This evidence indicates that these neurons have similar biophysical properties in terms of current density and kinetics of current development. The results shown in Figure 4h[1] have been already commented on above. Briefly, the protocol in Figure 4e[1] was applied on autaptic neurons chronically treated for 1 h with vehicle (used as control) or with Con-G′*-AuNPs **1**. Therefore, these experiments served to test the effect of a much longer incubation time with the nanoparticles on the observed antagonism. These experiments were run independently on different cell preparations, with respect to those displayed in Figure 4g,[1] yet the (I3 − I2)/I3 values (both are for cells treated with Con-G′*-AuNPs **1**) agree well with each other within the experimental error.

Finally, the criticism expressed in the comment about the comparison between two different types of conopeptide-functionalized AuNPs (Con-G′*-AuNPs **1** and Con-R′*-AuNPs **3**) and the conclusions we reached in our study is not founded, as we never made such comparisons. Indeed, we stated "*... our results show that both Con-G′*-AuNPs**1**and Con-R′*-AuNPs**3**protect neurons from excitotoxicity induced by a NMDA-bath application at a comparable concentration range (Figure 5a,c). Although, a more stringent comparison (based on a statistical analysis) is not possible, because of the chosen experimental design for the excitotoxicity experiments, this observation corroborates the electrophysiology recordings that showed AuNPs**1**and**3**as equally effective in antagonizing extrasynaptic NMDAR currents (Figure 4b,g). Overall, these results are consistent with the hypothesis that extrasynaptic NMDARs are predominantly GluN2B-containing di-heteromeric channels, at least in primary hippocampal neurons at 12−15 DIV ...*"

Pharmacological Characterization. There are well-established records of the NMDAR antagonist activity of Con-G and Con-R in the submicromolar to low micromolar range,[28−33] including on cultured hippocampal neurons.[34] Our nanoparticles are multivalent objects, that is, they allow presentation of many antagonist molecules in close vicinity of a NMDAR because tethered to the same nanoparticle, a phenomenon called *forced proximity*. Thus, the chosen peptide loading results in high local concentration of peptides in the millimolar range and can antagonize all NMDARs that can be physically reached by the nanoparticles, irrespective of the used nanoparticle concentration. Experiments at 0.25 nM are therefore meaningful to provide experimental evidence that Con-G-AuNPs do not block synaptic NMDA, while the same concentration does provide significant inhibition of total (synaptic + extrasynaptic) NMDA-gated currents, as demonstrated by two independent experimental protocols. Thus, it can be concluded that our nanoparticle-based antagonists must carry out their action at extrasynaptic NMDARs.

While determining experimentally the IC_{50} for a potential drug is important, it has the obvious limitation of being restricted to the specific system under investigation (for instance, peptide conjugation, nanoparticle nature, *etc.*). These experiments will be necessary for translation of our findings into therapy, but we have suggested in the manuscript that they should be performed on a system closer to a potential therapeutic application, and this was beyond the scope of the research described in our article. Indeed, we openly stated: "*... it is probable that nanoparticles of a biodegradable material, with a design that recapitulates the features of our AuNPs, will be chosen to translate these results into therapy*".[1]

Summing up, our study provides evidence that conopeptide-functionalized AuNPs exert anti-excitotoxic activity, even at "low" concentrations, by (partially) antagonizing only extrasynaptic NMDAR receptors. The great concern expressed in the comment by Molokanova *et al.* about the different concentrations used in electrophysiology *vs* neuroprotection experiments is totally unjustified. As a matter of fact, electrophysiology recordings were performed at 0.25 nM, while neuroprotection experiments were performed at 0.1, 0.5, and 1 nM. The results show that Con-G′*-AuNPs **1** at ≥0.5 nM and Con-R′*-AuNPs **3** at ≥0.1 nM (but not control AuNPs **2**) confer statistically significant neuroprotection to NMDA-treated neurons.

Neuroprotection. Most of the concerns expressed in this part of the comment by Molokanova *et al.* have been already addressed, including: (1) structural stability of the nanoconjugates, (2) choice of the nanoparticle concentration in both electrophysiology and neuroprotection experiments, and (3) absence of antagonistic activity at synaptic NMDARs. Some additional aspects will be discussed in the following paragraphs.

The first aspect concerns the alleged discrepancy between the results described in our recent manuscript and the data

https://doi.org/10.1021/acsnano.1c05607
ACS Nano 2021, 15, 15409−15417

reported in the Ph.D. thesis of Lisa Maus at the University of Heidelberg.[4] The Senior Author (Dr. Roberto Fiammengo) supervised the above-mentioned Ph.D. thesis, which focused on the development of the nanoparticles. At the end of her thesis (page 107 of 111 total, Figure 67[4]) submitted in 2010, Dr. Maus reported the results of few *preliminary* neuroprotection experiments run on *one* neuronal preparation with Con-G-functionalized nanoparticles. Unfortunately, treatment with the nanoparticles did not result in observable neuroprotection from NMDA-induced excitotoxicity. However, even for the treatment with soluble Con-G (Figure 65[4]), large variability was observed depending on the culture preparation, as explicitly noted in the thesis (page 105[4]). Thus, the results shown in Figure 67[4] cannot be used for any quantitative comparison or conclusion and were only reported to illustrate the work performed, the problems encountered, and a possible outlook for the considerable effort in nanoparticle development. Accordingly, in the "summary and outlook" paragraph on page 113, it is written: "*In ersten Zelltoduntersuchungen in dem primären System der hippocampalen Neuronen kann die Funktionalität der Peptid-Nanopartikel-Konjugate bisher nicht bestätigt werden*",[4] which translates literally to "*In initial cell-death experiments on primary hippocampal neurons it was not possible to confirm the functionality of the peptide-nanoparticle conjugates*". The project came to a prolonged stop due to relocation of the involved researchers, and a full-scale survival study (four experiments) was performed in 2015−2017 in collaboration with Imperial College London demonstrating neuroprotection by conopeptide-functionalized nanoparticles.

Notably, the experiments with hippocampal neurons described in Maus's Ph.D. thesis were performed on neuronal preparations that are substantially different compared to the ones used for the experiments reported in our article. In the first case, postnatal neurons cultures in the presence of serum with no inhibitors of glia proliferation were used (Ph.D. thesis, page 131[4]), while, in the second case, embryonic neurons cultures in serum-free conditions were used.[1] Due to the concomitant absence of glia proliferation inhibitors and the presence of serum, neuronal populations at 10−12 DIV inevitably contain a larger fraction of (dendro)glial cells, which have a very high survival rate and whose presence affects the survival of neurons. This effect is especially pronounced in postnatal neuron-glia cultures, as postnatal hippocampi have a higher glia content compared to the prenatal ones. Importantly, these two cell types are not discriminated by Hoechst. This fact may provide an additional explanation of why, in Maus' Ph.D. thesis, NMDA had a very variable effect on cell survival, and no significant effect of AuNP on survival was observed.

The second aspect we would like to address is the unjustified claim that the neuroprotection experiments were not properly performed. We appreciate that a few details may have not been immediately obvious from the Materials and Methods section of our *ACS Nano* article, and we are providing here an extensive explanation of the experimental design especially for researchers and readers who are less familiar with the field of neurobiology.

The methods we used are described in the two articles we referred to in the Materials and Methods section of our article, where we stated "*Analysis of neuronal survival was performed as previously described* (70, 71)".[1] Ref 71, a *Brain* article reports explicitly: "*Hippocampal neurons were plated at a density of 5 × 10*^{4}*cells per well in poly-L-lysine-coated eight-well LabTek Permanox slides (Nunc) ...*", *i.e.*, coverslips were not used at all in our neuroprotection experiments. And also: "*... At least 1000 cells/condition were recorded in a systematic series of view fields, with the position of the first field chosen randomly as described in Ronn et al. Cell viability was estimated based on nuclear morphology (dead cells displaying condensed chromatin or fragmented nuclei) in a semi-automatic mode using software developed at the laboratory to minimize bias*"."*... Results are presented as the mean of the live cell ratio [n live cells/(n live cells + ndead cells)*". In our *ACS Nano* article, we have also specified: "*For each antagonist (AuNP or peptide), one experiment consisted of testing the complete series of conditions on sibling cultures (untreated, 50 μM NMDA, 50 μM NMDA + indicated antagonist concentration, antagonist-only at the maximal concentration)*".[1] To clarify further, for each antagonist, one independent experiment represented one 8-well slide from one neuronal preparation. Neurons were taken from the same suspension and plated into the adjacent wells of the slide (sibling cultures). Thereafter, a series of conditions were tested on the same slide (with the maximal number of conditions, including untreated and NMDA-only treated cells, being eight). Such a multiwell design is a commonly accepted way of performing neurotoxicity studies as, in contrast to coverslips, it ensures that cells are plated uniformly and that fixation, staining, and mounting are identical within the series on the same slide. Each slide, along with multiple antagonist concentrations, contained untreated and NMDA-only treated controls, which were used for the subsequent ANOVA analysis.

As also stated in ref 71 of our manuscript, the acquired images were processed in a semi-automated mode using a laboratory-developed software (ImageJ based) to minimize bias. It is well-known that absolute dead cell counts in automated processing depend on several parameters, such as staining intensity, presence of cell debris/fragments, and contrast/thresholding[35,36] and may be slightly overestimated for preparations containing fragmented nuclei, as fragments may be detected as separate dead cells. However, since treatments within the series are stained and counted identically using the same software parameters, semi-automated processing allows to obtain low data variation, robust difference between positive and negative controls, and good reproducibility of results, whereas interobserver variations in manually processed viability data can reach 40%.[36] Moreover, single-stain cell counts are only reliable as relative (*i.e.*, treated *vs* control)[36] measures of neurotoxicity. Counts are therefore often normalized to untreated controls,[37,38] while in the current manuscript, we did show the unnormalized data, providing complete experimental information. The applied statistical analysis matches the experimental design, whereby all treatments within one series are processed identically including both positive and negative controls in each series.

Four to five separate neuronal preparations (4−5 pregnant rats) were used for each antagonist, each preparation allowing to independently test 4−6 different antagonists (1 experiment per antagonist), depending on cell yield. Therefore, for each antagonist, four independent experiments represent four complete series of conditions tested in four independent neuronal preparations from four different animals (pregnant rats), each series tested in a separate 8-well slide. Thus, the remark in Molokanova's comment "*... one may assume that all "independent" neuroprotective experiments were conducted on only one neuronal preparation*" is unfounded. Additionally, performing all neuroprotective experiments on one neuronal

https://doi.org/10.1021/acsnano.1c05607
ACS Nano 2021, 15, 15409−15417

preparation is physically impossible, as it would require *ca.* 40 slides = 16 × 10^6 neurons. It is a well-known fact for researchers working with embryonic hippocampal cultures that this is a totally unrealistic amount for one E19 pregnant Wistar rat with the normal neuronal yield of approximately 1 × 10^6 neurons per fetus.

As previously shown by numerous laboratories, including ours, Hoechst staining is a robust method to evaluate cytotoxicity, especially in cases involving modest excitotoxic insults mostly inducing cell apoptosis, such as in our present *ACS Nano* paper. We referred readers to our previous *Nature Communications* article,[37] where Hoechst staining was indeed used to evaluate cytotoxicity/neuroprotection in cultured hippocampal neurons following oxidative stress and excitotoxic challenge. The results (Figures 1e and 3d,e[37]) were validated in parallel *in vivo* studies described in the same article (five different in vivo models including two models of excitotoxicity and seven different stainings including cresyl violet, 8-oxoguanine, and TUNEL),[37] fully confirming the *in vitro* neuroprotection data. We also referred the readers to our *Brain* paper,[38] where we used the same Hoechst-based protocol to evaluate the protective effect of a neurotrophic peptide in cultured hippocampal neurons subjected to excitotoxicity (Figure 5[38]). Again, the validity of this approach was confirmed by a parallel study *in vivo* using H&E and Fluoro-Jade stainings (Figure 8[38]).

The third aspect we would like to shortly address is about the structural design of our antagonist-nanoparticle conjugates. The comment suggests, without any supporting scientific evidence, that our alkyl-PEG600 thiols could cause limited antagonist freedom being "fairly short" and, for the same reason, may cause colloidal instability. In our *ACS Nano* article in 2010,[3] we have already clearly demonstrated that these nanoparticles do not aggregate even in 2 M NaCl, exactly like nanoparticles coated with PEG3000 derivatives, which are closer to the ones used by Molokanova *et al.* They also do not aggregate in the cell culture medium used for hippocampal neuron culture in our manuscript (see Figure 2). We have also shown that they can bind selectively to NMDARs recombinantly expressed by transfected HEK 293 cells,[3] and our 2020 article[1] fully supports the antagonism at NMDA receptors. The comment also completely ignores that several other laboratories have independently confirmed that the presence of an alkyl chain of 11 carbons between the thiol group and the PEG segment is beneficial to the overall stabilization of the SAMs (see above Stability of the Passivation Layer section).[6−8,39] One of these studies reported the analysis of the protein corona of AuNPs passivated with alkyl-PEG600 thiols, concluding that such nanoparticles have very little protein corona and reduced propensity to form intracellular aggregates outperforming AuNPs passivated with PEG5000.[7] However, the formation of a protein corona on our nanoparticles cannot be completely ruled out, since our system differs from the one investigated in the literature[7] because peptides are attached to the passivation layer made of alkyl-PEG600 thiols. To account for any potential impact of protein corona, we have prepared control nanoparticles (Ctrl AuNPs **2**) that were functionalized with a comparable number of peptides (called Ctrl pept*) with the same sequence of Con-G*, except that all five γ-carboxyglutamate residues were replaced by isoglutamates (γE, see Chart 1[1]). Our results show that Con-G*-AuNPs **1** (and Con-R′*-AuNPs **3**) have a significant antagonist activity compared to Ctrl AuNPs **2**, suggesting that if any protein corona is formed, it must be a "soft" protein corona,[40] which allows interaction between the conjugated peptides and the NMDA receptors.

Finally, concerning the dimerization capability of Con-G, while Castellino and co-workers observed NMDAR antagonist activity also for (some) Con-G dimers,[41,42] they never concluded dimers were necessary for activity.

ALTERNATIVE DESIGN OF EXCLUSIVE ENMDAR MODULATORS BY SAVCHENKO *ET AL.* (2016) AND SIDE-BY-SIDE COMPARISON

We completely agree on the importance of developing "*functionally-active neuroprotection-capable exclusive modulators of eNMDARs* (extrasynaptc NMDARs) ...", and we have acknowledged that the Molokanova group was the first achieving this goal. Our results are fully supportive of their observations. Considering that our antagonist-nanoparticle conjugates and those reported by Molokanova *et al.* do present some structural differences (nanoparticle core size, coating structure, conjugation chemistry and antagonist identity), the observation of analogous effects strongly supports the hypothesis on which these studies are based. The general conclusion of both studies is PEGylated, NMDAR antagonist-functionalized AuNPs, whose size is large enough to prevent their diffusion into the synapse, antagonize only (a fraction of) extrasynaptically located NMDARs, and are thereby neuroprotective. Indeed, we think it is rather reassuring to see that analogous effects can be independently observed in different laboratories. Contrary to the comment narrative, in our article, there is no language tending to disparage the design of the nanoparticles developed by the Molokanova group, since the two systems have several common characteristics as well as some differences. We offered the reader of our article a plain comparison based only on published data. In the meantime, it seems that the Molokanova group has acquired additional information about their system, especially *in vivo*, which could bring them closer to a therapeutic exploitation of their system. As E. Molokanova is a founder of NeurANO Bioscience, a company involved in research and development of nanotherapeutics for neurological disorders, we wish her a lot of success in this endeavor.

CONCLUSIONS

This response with in-depth discussion to the questions raised by Molokanova *et al.* in their comment should help the readers to better appreciate the methodology and the biological significance of the results described in our 2020 *ACS Nano* article.[1] We understand very well the concerns of neurologists about a possible utilization of nanoparticles in the brain, but our article is not meant to describe a new therapeutic drug. We are convinced that our system, as well as that developed by the Molokanova group, may contribute to a deeper understanding of the role of overactivation of extrasynaptic NMDARs in neurodegeneration.

AUTHOR INFORMATION

Corresponding Author

Roberto Fiammengo − *Center for Biomolecular Nanotechnologies@UniLe, Istituto Italiano di Tecnologia, Arnesano, Lecce 73010, Italy; Department of Biotechnology, University of Verona, Verona 37134, Italy;* orcid.org/

https://doi.org/10.1021/acsnano.1c05607
ACS Nano 2021, 15, 15409−15417

0000-0002-6087-6851; Email: roberto.fiammengo@univr.it

Authors

Pierluigi Valente − *Department of Experimental Medicine, School of Medical and Pharmaceutical Sciences, University of Genoa, Genoa 16132, Italy; IRCSS Ospedale Policlinico San Martino, Genoa 16132, Italy*

Darya Kiryushko − *Center for Neuroinflammation and Neurodegeneration, Imperial College London, London W12 0NN, United Kingdom; Department of Materials and London Center for Nanotechnology, Imperial College, London SW72AZ, United Kingdom;* orcid.org/0000-0001-5177-3669

Silvio Sacchetti − *Center for Synaptic Neuroscience and Technology, Istituto Italiano di Tecnologia, Genoa 16132, Italy*

Pedro Machado − *Centre for Ultrastructural Imaging, Kings College London, London SE1 1UL, United Kingdom*

Claire M. Cobley − *Department of Physical Chemistry, University of Heidelberg, Heidelberg 69120, Germany; Max Planck Institute for Intelligent Systems, Stuttgart 70569, Germany*

Vincenzo Mangini − *Center for Biomolecular Nanotechnologies@UniLe, Istituto Italiano di Tecnologia, Arnesano, Lecce 73010, Italy;* orcid.org/0000-0002-0743-2178

Alexandra E. Porter − *Department of Materials and London Center for Nanotechnology, Imperial College, London SW72AZ, United Kingdom;* orcid.org/0000-0002-9798-8398

Joachim P. Spatz − *Department of Physical Chemistry, University of Heidelberg, Heidelberg 69120, Germany; Max Planck Institute for Medical Research, Heidelberg 69120, Germany*

Roland A. Fleck − *Centre for Ultrastructural Imaging, Kings College London, London SE1 1UL, United Kingdom*

Fabio Benfenati − *IRCSS Ospedale Policlinico San Martino, Genoa 16132, Italy; Center for Synaptic Neuroscience and Technology, Istituto Italiano di Tecnologia, Genoa 16132, Italy;* orcid.org/0000-0002-0653-8368

Complete contact information is available at: https://pubs.acs.org/10.1021/acsnano.1c05607

Author Contributions

‡These authors contributed equally.

Funding

This study was supported by the European Community and the Italian Ministry of Health within the ERA-NET Euro-NanoMed3 "NanoLight" project (grant ID 2019-132), Fondazione Cariplo (project 2018-0505), Italian Ministry of Health (Ricerca Finalizzata GR-2016-02363972), Italian Ministry of Foreign Affairs (Farnesina—MAECI; grant no. MAE00694702021-05-20) to F.B., and IRCCS Ospedale Policlinico San Martino (Ricerca Corrente and "5x1000") to P.V. and F.B.

Notes

We have also submitted to the Editor: (1) the emails confirming that antagonists were fabricated and shipped in different batches with shipping dates ranging from 2015 to 2017, and (2) the intermediate report files with the last modification dates ranging from 2015 to 2017 which prove that the neuronal survival studies were conducted in five stages during the period of July, 2015 and June, 2017.

REFERENCES

(1) Valente, P.; Kiryushko, D.; Sacchetti, S.; Machado, P.; Cobley, C. M.; Mangini, V.; Porter, A. E.; Spatz, J. P.; Fleck, R. A.; Benfenati, F.; Fiammengo, R. Conopeptide-Functionalized Nanoparticles Selectively Antagonize Extrasynaptic *N*-Methyl-D-aspartate Receptors and Protect Hippocampal Neurons from Excitotoxicity In Vitro. *ACS Nano* **2020**, *14*, 6866−6877.

(2) Savchenko, A.; Braun, G. B.; Molokanova, E. Nanostructured Antagonist of Extrasynaptic NMDA Receptors. *Nano Lett.* **2016**, *16*, 5495−5502.

(3) Maus, L.; Dick, O.; Bading, H.; Spatz, J. P.; Fiammengo, R. Conjugation of Peptides to the Passivation Shell of Gold Nanoparticles for Targeting of Cell-Surface Receptors. *ACS Nano* **2010**, *4*, 6617−6628.

(4) Maus, L. Entwicklung Stabiler Gold Nanopartikel-Peptid-Konjugate zur Untersuchung von Rezeptor-Liganden Wechselwirkungen im Zellulären System. *Ph.D. Thesis*, Ruprecht-Karls-Universität Heidelberg, Heidelberg, 2010.

(5) Bading, H. Nuclear Calcium Signalling in the Regulation of Brain Function. *Nat. Rev. Neurosci.* **2013**, *14*, 593−608.

(6) Larson, T. A.; Joshi, P. P.; Sokolov, K. Preventing Protein Adsorption and Macrophage Uptake of Gold Nanoparticles via a Hydrophobic Shield. *ACS Nano* **2012**, *6*, 9182−9190.

(7) Silvestri, A.; Di Silvio, D.; Llarena, I.; Murray, R. A.; Marelli, M.; Lay, L.; Polito, L.; Moya, S. E. Influence of Surface Coating on the Intracellular Behaviour of Gold Nanoparticles: A Fluorescence Correlation Spectroscopy Study. *Nanoscale* **2017**, *9*, 14730−14739.

(8) Schulz, F.; Dahl, G. T.; Besztejan, S.; Schroer, M. A.; Lehmkühler, F.; Grübel, G.; Vossmeyer, T.; Lange, H. Ligand Layer Engineering to Control Stability and Interfacial Properties of Nanoparticles. *Langmuir* **2016**, *32*, 7897−7907.

(9) Prorok, M.; Castellino, F. J. The Molecular Basis of Conantokin Antagonism of NMDA Receptor Function. *Curr. Drug Targets* **2007**, *8*, 633−642.

(10) Maus, L.; Spatz, J. P.; Fiammengo, R. Quantification and Reactivity of Functional Groups in the Ligand Shell of PEGylated Gold Nanoparticles via a Fluorescence-Based Assay. *Langmuir* **2009**, *25*, 7910−7917.

(11) Jans, K.; Bonroy, K.; De Palma, R.; Reekmans, G.; Jans, H.; Laureyn, W.; Smet, M.; Borghs, G.; Maes, G. Stability of Mixed PEO-Thiol SAMs for Biosensing Applications. *Langmuir* **2008**, *24*, 3949−3954.

(12) Flynn, N. T.; Tran, T. N. T.; Cima, M. J.; Langer, R. Long-Term Stability of Self-Assembled Monolayers in Biological Media. *Langmuir* **2003**, *19*, 10909−10915.

(13) Luk, Y.-Y.; Kato, M.; Mrksich, M. Self-Assembled Monolayers of Alkanethiolates Presenting Mannitol Groups Are Inert to Protein Adsorption and Cell Attachment. *Langmuir* **2000**, *16*, 9604−9608.

(14) Vauquelin, G.; Charlton, S. J. Exploring Avidity: Understanding the Potential Gains in Functional Affinity and Target Residence Time of Bivalent and Heterobivalent Ligands. *Br. J. Pharmacol.* **2013**, *168*, 1771−1785.

(15) Tassa, C.; Duffner, J. L.; Lewis, T. A.; Weissleder, R.; Schreiber, S. L.; Koehler, A. N.; Shaw, S. Y. Binding Affinity and Kinetic Analysis of Targeted Small Molecule-Modified Nanoparticles. *Bioconjugate Chem.* **2010**, *21*, 14−19.

(16) Hong, S.; Leroueil, P. R.; Majoros, I. J.; Orr, B. G.; Baker, J. R.; Banaszak Holl, M. M. The Binding Avidity of a Nanoparticle-Based Multivalent Targeted Drug Delivery Platform. *Chem. Biol.* **2007**, *14*, 107−115.

(17) Krishnamurthy, V. M.; Estroff, L. A.; Whitesides, G. M. Multivalency in Ligand Design. In *Fragment-Based Approaches in Drug Discovery*; Wiley-VCH Verlag GmbH & Co. KGaA: Weinheim, **2006**; pp 11−53.

(18) Ogden, K. K.; Traynelis, S. F. New Advances in NMDA Receptor Pharmacology. *Trends Pharmacol. Sci.* **2011**, *32*, 726−733.

(19) Bastús, N. G.; Comenge, J.; Puntes, V. Kinetically Controlled Seeded Growth Synthesis of Citrate-Stabilized Gold Nanoparticles of up to 200 nm: Size Focusing versus Ostwald Ripening. *Langmuir* **2011**, *27*, 11098−11105.
(20) Sykes, E. A.; Chen, J.; Zheng, G.; Chan, W. C. W. Investigating the Impact of Nanoparticle Size on Active and Passive Tumor Targeting Efficiency. *ACS Nano* **2014**, *8*, 5696−5706.
(21) Parsons, M. P.; Raymond, L. A. Extrasynaptic NMDA Receptor Involvement in Central Nervous System Disorders. *Neuron* **2014**, *82*, 279−293.
(22) Benke, T. A.; Jones, O. T.; Collingridge, G. L.; Angelides, K. J. *N*-Methyl-D-Aspartate Receptors Are Clustered and Immobilized on Dendrites of Living Cortical Neurons. *Proc. Natl. Acad. Sci. U. S. A.* **1993**, *90*, 7819−7823.
(23) Lorber, B.; Fischer, F.; Bailly, M.; Roy, H.; Kern, D. Protein Analysis by Dynamic Light Scattering: Methods and Techniques for Students. *Biochem. Mol. Biol. Educ.* **2012**, *40*, 372−382.
(24) Zuber, B.; Nikonenko, I.; Klauser, P.; Muller, D.; Dubochet, J. The Mammalian Central Nervous Synaptic Cleft Contains a High Density of Periodically Organized Complexes. *Proc. Natl. Acad. Sci. U. S. A.* **2005**, *102*, 19192.
(25) Lučić, V.; Yang, T.; Schweikert, G.; Förster, F.; Baumeister, W. Morphological Characterization of Molecular Complexes Present in the Synaptic Cleft. *Structure* **2005**, *13*, 423−434.
(26) Nance, E. A.; Woodworth, G. F.; Sailor, K. A.; Shih, T. Y.; Xu, Q.; Swaminathan, G.; Xiang, D.; Eberhart, C.; Hanes, J. A Dense Poly(ethylene glycol) Coating Improves Penetration of Large Polymeric Nanoparticles Within Brain Tissue. *Sci. Transl. Med.* **2012**, *4*, 149ra119.
(27) McKay, S.; Bengtson, C. P.; Bading, H.; Wyllie, D. J. A.; Hardingham, G. E. Recovery of NMDA Receptor Currents from MK-801 Blockade Is Accelerated by Mg2+ and Memantine under Conditions of Agonist Exposure. *Neuropharmacology* **2013**, *74*, 119−125.
(28) Donevan, S. D.; McCabe, R. T. Conantokin G Is an NR2B-Selective Competitive Antagonist of *N*-Methyl-D-Aspartate Receptors. *Mol. Pharmacol.* **2000**, *58*, 614−623.
(29) Barton, M. E.; Steve White, H.; Wilcox, K. S. The Effect of CGX-1007 and CI-1041, Novel NMDA Receptor Antagonists, on NMDA Receptor-Mediated EPSCs. *Epilepsy Res.* **2004**, *59*, 13−24.
(30) Ragnarsson, L.; Yasuda, T.; Lewis, R. J.; Dodd, P. R.; Adams, D. J. NMDA Receptor Subunit-Dependent Modulation by Conantokin-G and Ala(7)-Conantokin-G. *J. Neurochem.* **2006**, *96*, 283−291.
(31) Alex, A. B.; Baucum, A. J.; Wilcox, K. S. Effect of Conantokin G on NMDA Receptor-Mediated Spontaneous EPSCs in Cultured Cortical Neurons. *J. Neurophysiol.* **2006**, *96*, 1084−1092.
(32) White, H. S.; McCabe, R. T.; Armstrong, H.; Donevan, S. D.; Cruz, L. J.; Abogadie, F. C.; Torres, J.; Rivier, J. E.; Paarmann, I.; Hollmann, M.; Olivera, B. M. *In Vitro* and *In Vivo* Characterization of Conantokin-R, a Selective NMDA Receptor Antagonist Isolated from the Venom of the Fish-Hunting Snail *Conus Radiatus*. *J. Pharmacol. Exp. Ther.* **2000**, *292*, 425.
(33) Sheng, Z.; Dai, Q.; Prorok, M.; Castellino, F. J. Subtype-Selective Antagonism of *N*-methyl-D-aspartate Receptor Ion Channels by Synthetic Conantokin Peptides. *Neuropharmacology* **2007**, *53*, 145−156.
(34) Klein, R. C.; Galdzicki, Z.; Castellino, F. J. Inhibition of NMDA-Induced Currents by Conantokin-G and Conantokin-T in Cultured Embryonic Murine Hippocampal Neurons. *Neuropharmacology* **1999**, *38*, 1819−1829.
(35) Schwendy, M.; Unger, R. E.; Bonn, M.; Parekh, S. H. Automated Cell Segmentation in FIJI® Using the DRAQ5 Nuclear Dye. *BMC Bioinf.* **2019**, *20*, 39.
(36) Maidana, D. E.; Tsoka, P.; Tian, B.; Dib, B.; Matsumoto, H.; Kataoka, K.; Lin, H.; Miller, J. W.; Vavvas, D. G. A Novel ImageJ Macro for Automated Cell Death Quantitation in the Retina. *Invest. Ophthalmol. Visual Sci.* **2015**, *56*, 6701−6708.
(37) Dmytriyeva, O.; Pankratova, S.; Owczarek, S.; Sonn, K.; Soroka, V.; Ridley, C. M.; Marsolais, A.; Lopez-Hoyos, M.; Ambartsumian, N.; Lukanidin, E.; Bock, E.; Berezin, V.; Kiryushko, D. The Metastasis-Promoting S100A4 Protein Confers Neuroprotection in Brain Injury. *Nat. Commun.* **2012**, *3*, 1197.
(38) Pankratova, S.; Kiryushko, D.; Sonn, K.; Soroka, V.; Køhler, L. B.; Rathje, M.; Gu, B.; Gotfryd, K.; Clausen, O.; Zharkovsky, A.; Bock, E.; Berezin, V. Neuroprotective Properties of a Novel, Non-Haematopoietic Agonist of the Erythropoietin Receptor. *Brain* **2010**, *133*, 2281−2294.
(39) Schulz, F.; Vossmeyer, T.; Bastús, N. G.; Weller, H. Effect of the Spacer Structure on the Stability of Gold Nanoparticles Functionalized with Monodentate Thiolated Poly(ethylene glycol) Ligands. *Langmuir* **2013**, *29*, 9897−9908.
(40) Mohammad-Beigi, H.; Hayashi, Y.; Zeuthen, C. M.; Eskandari, H.; Scavenius, C.; Juul-Madsen, K.; Vorup-Jensen, T.; Enghild, J. J.; Sutherland, D. S. Mapping and Identification of Soft Corona Proteins at Nanoparticles and Their Impact on Cellular Association. *Nat. Commun.* **2020**, *11*, 4535.
(41) Dai, Q.; Sheng, Z.; Geiger, J. H.; Castellino, F. J.; Prorok, M. Helix-Helix Interactions between Homo- and Heterodimeric 4-Carboxyglutamate-containing Conantokin Peptides and Their Derivatives. *J. Biol. Chem.* **2007**, *282*, 12641−12649.
(42) Sheng, Z.; Prorok, M.; Castellino, F. J. Specific Determinants of Conantokins That Dictate Their Selectivity for the NR2B Subunit of *N*-methyl-D-aspartate Receptors. *Neuroscience* **2010**, *170*, 703−710.

https://doi.org/10.1021/acsnano.1c05607
ACS Nano 2021, 15, 15409−15417